



Annular liquid film thickness prediction in a vertical 180° return bend

M. Abdulkadir^{a,*}, J.N. Samson^b, D. Zhao^c, D.U. Okhiria^d, V. Hernandez-Perez^e

^a Department of Chemical Engineering, Federal University of Technology, Minna, Niger State, Nigeria

^b Department of Chemical Engineering, University of Abuja, Nigeria

^c School of Engineering, London South Bank University, London, United Kingdom

^d Department of Chemical and Petroleum Engineering, Federal University Ndufu-Alike Ikwo, (FUNAI), Abakaliki, Ebonyi State, Nigeria

^e Department of Mechanical Engineering, Faculty of Engineering, National University of Singapore, Singapore

ARTICLE INFO

Keywords:

Liquid film thickness
Annular flow
180-degree bend
Prediction
Air–water
Dimensionless numbers

ABSTRACT

Annular flow is predominant in gas wells. Liquid may be present in form of entrained droplets as well as in the liquid film on pipe wall. The knowledge of the average liquid film thickness is vital for detailed mechanistic modelling of churn–annular flow in engineering applications. So far, the models for liquid film thickness prediction are limited to vertical and horizontal pipes. These models were based on limited ranges of experimental data. In addition, exhaustive iterations are needed when these models are used to estimate liquid film thickness. In this work, a new correlation to predict liquid film thickness in a 180° bend under gas–liquid annular conditions was successfully proposed. The correlation was based on dimensionless numbers (modified gas and liquid Weber numbers and gas Froude number) which reflect the underlined physics governing gas–liquid interaction in the bend. The Weber numbers capture the two important forces (inertial and surface tension forces) which govern the formation of the liquid film thickness within the system while gas Froude number quantifies the interaction of two important forces (centrifugal and gravitational forces) which determines the distribution of the phases across a bend. The proposed liquid film thickness correlation was based on the experimental data obtained from a wide range of operating conditions. The liquid superficial velocities ranges from 0.02 to 0.2 m/s and gas superficial velocities from 3.5 to 16 m/s at different measurement locations of 45°, 90° and 135° of the bend with a diameter of 127 mm. The liquid film thickness in air–water and helium–water annular flow can be predicted by $\delta = 28.4061(We_L)^{0.10318}(We_G)^{-0.30954}(Fr_G)^{-0.31423}$. The validation of the proposed correlation used to predict liquid film thickness in gas–liquid annular systems with different pipe diameters were examined against the available data in the literature. Good agreement was found between the predicted values of liquid film thickness with the experimental data at different measuring locations of the bend.

1. Introduction

In oil and gas production systems, pipe fittings such as elbows and tees are commonly used. Such fittings are usually prone to corrosion most especially if sand particles are present in the flowing fluid and these failures have in the past resulted in great financial and human losses [37]. The presence of the liquid film in the pipe bend in an annular flow serves to cushion the impact of these sand particles on the pipe wall. Also, in process industries, annular gas–liquid flow across a bend is common in equipment such as the boilers and due to the asymmetric distribution of the liquid film thickness, the heat transfer mechanism will be grossly affected resulting in a burn-out and equipment damage [13]. Therefore, to better design these processes, it is important to develop a correlation that can accurately predict the liquid film thickness distribution across the bend using easy access input

parameters such as gas and liquid physical properties and superficial velocities.

Annular flow is one of the predominantly encountered flow patterns in a number of industrial applications such as nuclear reactors, oil and gas production, steam generations etc. [3]. Annular gas–liquid flow pattern usually occurs at a high gas flow rate and low liquid flow rate where the liquid forms a film around the wall of the pipe, while the gas flows within the core with some liquid droplets entrained in it. The study of the behaviour of this tiny liquid film around the internal walls of the pipe, most especially in a curve pipe, is so important in understanding complex phenomena such as prediction of erosion magnitude within pipe bends, heat transfer regimes in heating processes, etc. [31].

According to Usui et al. [42], gas–liquid flow in curved channels usually involves the combined action of forces which tend to produce such complications as inhomogeneous phase distribution, flow reversal,

* Corresponding author.

E-mail address: mukhau@futminna.edu.ng (M. Abdulkadir).

flooding, secondary flow and coalescence. These effects can lead to corrosion, burn-out and subsequent tube failure. Thus, the hydrodynamic behaviour of a two-phase mixture flowing through curved channels is of prime importance to designers. Abdulkadir et al. [3] reported that several experimental studies have been done on multiphase flow across 180° pipe bends such as the works done by Oshinowo and Charles [30], Anderson and Hills [7,43], Wang et al. [44,45]. Also, Tkaczyk and Morvan [40] reported that several authors have investigated numerically the gas–liquid flow in bends and have been able to develop some models. However, all those models were limited to bubbly flow regime where the gas exists as bubbles dispersed in the continuous liquid phase.

Gas–liquid flow across a 90° bend has also been studied experimentally by Schubring et al. [37], Abdulkadir et al. [2], Saidj et al. [33] and others. On the matter of annular flow, Zahedi et al. [46] developed a correlation to predict the liquid film thickness in a 90° elbow. Their correlation was based on the liquid film correlations of Kosky [25], Asali et al. [9] and Ambrosini et al. [6] for an annular flow in a vertical flow. But according to MacGillivray [27], these correlations are not very practical for design purposes since they require either the knowledge or calculation of entrainment (to calculate the liquid film mass flow rate) or the shear stress (to calculate the friction velocity). These two quantities are not readily available from experimental work and must be calculated with further empirical or semi-empirical correlations. Zahedi et al. [46] proposed a correlation to predict liquid film thickness. Unfortunately their correlation was based on Reynolds Number and did not fully capture the interplay of the centrifugal and gravitational forces that directly influences the liquid film thickness in a bend. They recommended that other additional terms be added in the model.

It is in view of this background that a new correlation will be developed. The correlation will be able to predict the liquid film thickness from the knowledge of fluid flow rates and other phase parameters without having to use empirical correlations to calculate the entrainment and friction velocity and also a model that fully captures the dynamics of the flow forces at work in a bend.

2. Literature review

2.1. Two-phase gas–liquid flow in a 180° bend

According to Ribeiro [32], experimental observations made by different researchers have shown that two-phase flow patterns in a bend are qualitatively the same as those seen in a straight pipe and that the presence of a bend introduces a developing situation in the flow pattern whereby the relative positions and the flow velocities of the phases are redistributed. For air–water flow round a vertical 90° bend, Gardner and Neller [20] suggested that the phase distribution is governed by the competing centrifugal force, which tend to take the liquid to the outside of the bend and gravity which causes the liquid to fall to the inside of the bend. They suggested that the ratio of the centrifugal and gravitational forces can be represented by the modified Froude number given as:

$$Fr_{\theta} = \frac{u_M^2}{rg \sin \theta} \quad (1)$$

where r , g , u_M and θ are the radius of the bend, acceleration due to gravity, mixture superficial velocity and angle of the bend, respectively.

Using the numerical value of the modified Froude number, Eq. (1), an attempt to explain the distribution of the phases within the bend was put forward by them. They discovered that if the value of the modified Froude number is greater than unity, the air will flow towards the inside of the bend but if the value is less than unity, the air will flow towards the outside of the bend and that if the value of the modified Froude number is equal to unity, the both phases will be in radial

equilibrium [1].

Along the same line of reasoning Oshinowo and Charles [30] and Usui et al. [41,42], gave a qualitative discussion on the interaction between centrifugal force and gravity for a flow about a bend axis. They explained this interaction by proposing a modified form of Froude's number expressed in terms of the actual velocities for both the liquid and gas.

$$Fr_{\theta} = \frac{v_L^2}{\left(\frac{\rho_L - \rho_G}{\rho_L}\right) r g \sin \theta} \left[1 - \frac{\rho_G v_G^2}{\rho_L v_L^2} \right] \quad (2)$$

where ρ_G and ρ_L are the densities of the gas and liquid, respectively; v_G and v_L are the actual velocity of gas and liquid, respectively.

In agreement with the explanation put forward by Gardner and Neller [20], they explained that if the left-hand side of Eq. (2) is greater than 1, then the liquid will move to the outside of the bend and if it is less than 1, the liquid will move inside the bend.

Usui et al. [41] investigated the flow behaviour and phase distribution in two-phase flow around an inverted U-bend using 24 mm internal diameter tubing. They were able to measure the distribution of local void fraction along a diameter lying in the central plane of the bend and over the whole cross-section of bend tube.

Almabrok et al. [5] carried out experiments to study gas–liquid two phase flow behaviours in upward and downward vertical pipes connected to a 180° bend. They observed that centrifugal force present in the 180° bend caused a flow mal-distribution in the adjacent straight section. In addition, they also noted from the time trace and the PDF of void fraction results that the gas superficial velocity has obvious effects on the flow development along different positions of the pipes. Oliveira and Barbosa [29] investigated the nature of the developing flow upstream and downstream of a vertical 180° return bend (curvature radius of 8.7) by means of void fraction and pressure drop measurements at several positions along the 26.4 mm internal diameter tubes connected to the bend. They were able to evaluate the effect of the bend on the flow characteristics for the plug, slug and annular flow regimes.

Gas–liquid flow behaviour in a 90° bend is different from that in a 180° bend. This will be discussed in the following section.

2.2. Flow regimes in bends

When a gas–liquid mixture flow in a tube, the flow phases may distribute in a variety of patterns. In order to determine the flow characteristics such as the pressure drop or liquid film thickness, it is important to first know the flow regimes present for the given flow conditions [19]. The presence of bends in a flow system usually affects the flow configurations and structures of upstream, downstream and within the bend. For instance, in a vertically positioned bend, there is usually an inter play of centrifugal, gravitational and buoyancy forces which leads to complicated flow behaviour such as inhomogeneous phase distribution, flow reversal, flooding, secondary flow and coalescence [33]. The understanding of the flow behaviour upstream, through and downstream of the bend is of prime importance in the design of the devices where they are present. Abdulkadir et al. [2] analysed the effects of the 90° bends on two-phase air–silicone oil flow using advanced instrumentation, electrical capacitance tomography (ECT), wire mesh sensor (WMS) and high speed video camera. They used the cross-sectional average void fraction data to identify the flow patterns upstream and downstream of the bend and found that bubble, stratified, slug and semi-annular flow patterns were present downstream of the vertical 90° bend whilst for the horizontal 90° bend, the flow pattern exhibited the same configurations as upstream of the bend. They concluded that the liquid flow rate has an insignificant effect on the two-phase flow behaviour for the upstream section of the vertical 90° bend and that the flow patterns are predominantly cap bubble, slug, unstable slug, and churn flows.

2.3. Liquid film thickness in vertical gas–liquid annular flow

Liquid film thickness in vertical annular gas–liquid flow has been examined extensively in the literature. Kosky [25] was one of the first authors to develop a correlation to determine the liquid film thickness for vertical upward flows in straight section of pipes. He derived the dimensionless liquid film thickness, δ^+ , as a function of liquid film Reynolds number from Prandtl's 1/7th power law velocity profile for turbulent flows as:

$$\delta^+ = 0.0504Re_{lf}^{0.875} \quad (3)$$

where Re_{lf} is the liquid film Reynolds number.

Asali et al. [9] later improved Kosky [25]'s correlation for $20 < Re_{lf} < 300$ using experimental data and proposed Eq. (4):

$$\delta^+ = 0.34Re_{lf}^{0.6} \quad (4)$$

Several years later, Ambrosini et al. [6] collected a wide range of experimental data by varying the pipe diameter and the working fluid used and was able to develop a correlation based on that of Kosky [25] and Asali et al. [9] and reported that the transition between these two correlations is at $Re_{lf} = 1000$ and that the empirical equations for the liquid film thickness are correlated with the liquid film Reynolds number, Eq. (5):

$$\delta^+ = ARe_{lf}^B \quad (5)$$

For the correlation of Asali et al. [9], 0.34 and 0.6 represent the constants A and B, respectively within $Re_{lf} \leq 1000$ while on the other hand 0.0512 and 0.875 represents the constants A and B, respectively within $Re_{lf} > 1000$ for the Kosky [25] correlation.

Fukano and Furukawa [18] developed a correlation for vertical upward flows based on annular flow data collected during an experiment where the fluid used are air–water and air–glycerine solutions in a 19 mm and 26 mm tubes, respectively. The correlation is reported to be able to predict mean film thickness to within 15% for the entire range of data and it is given as:

$$\frac{\delta}{D} = 0.0594e^{(-0.34Fr_G^{0.25}Re_{SL}^{0.19}x^{0.6})} \quad (6)$$

where Fr_G is the gas Froude number, Re_{SL} is the liquid superficial Reynolds number and x is the gas quality. The gas Froude number can be calculated from:

$$Fr_G = \frac{u_{SG}}{\sqrt{gD}} \quad (7)$$

where

g is the acceleration due to gravity.

The liquid superficial Reynolds number is calculated using:

$$Re_{SL} = \frac{u_{SL}D\rho_L}{\mu_L} \quad (8)$$

The gas quality, x , is the ratio between the mass flow rate of the gas (m_G) and the total mass flow rate of the gas–liquid mixture ($m_G + m_L$) and can be calculated using Eq. (9)

$$X = \frac{m_G}{m_G + m_L} = \frac{u_{SG}\rho_G}{u_{SG}\rho_G + u_{SL}\rho_L} \quad (9)$$

MacGillivray [27] equally developed a liquid film thickness correlation based on the work done by de Jong [16]. He plotted the combined data for helium–water and air–water systems at a pressure of 18 MPa in a 9.525 mm internal diameter pipe as one data set to obtain the new correlation which is given as:

$$\frac{\rho_L u_{SL} \delta}{\mu_L} = 39Re_{SL}^{0.2} \left(\frac{x}{1-x} \right)^{-1.0} \left(\frac{\rho_G}{\rho_L} \right)^{0.5} \quad (10)$$

Berna et al. [11] used a wide range of data to develop another correlation for the liquid film thickness taking into consideration the physical properties of the working fluids and the conditions of the experiments such as the gas and liquid superficial velocities, densities and dynamic viscosities for both fluids and the surface tension of the liquid phase. The correlation that they proposed is:

$$\frac{\delta}{D} = 7.165Re_G^{-10.07}Re_{SL}^{0.48} \left(\frac{Fr_G}{Fr_L} \right)^{0.24} \quad (11)$$

2.4. Liquid film thickness in bends

In the study of gas–liquid annular flow in a bend, it has been discovered that the variation of the liquid film thickness around the pipe circumference is quite complex. Several research works have been performed over the years to elucidate the dynamics of the liquid film thickness and its relationship with other hydrodynamic flow parameters in order to assist in the accurate design of the numerous gas–liquid annular systems involving bends. Abdulkadir [1] stated that in bends, the moving direction of the liquid film depends on the relative magnitude of the pressure, interfacial shear, centrifugal and gravity forces which act in a combined manner to induce secondary flow in the liquid film. Also, under the condition where the momentum of the gas phase is higher than the momentum of the liquid phase, the maximum liquid film thickness is seen to be displaced to the inside of the bend. Several authors have investigated experimentally the effects of the bend on the liquid film distribution in a gas–liquid annular flow.

Anderson and Hills [7] used an inverted U-tube return bend to study parameters such as liquid film thickness, gas velocity distribution and droplet entrainment in an annular flow using a pipe bend of 25 mm internal diameter and radius of curvature of 305 mm. In their work, they observed an increase in the liquid film thickness in the inside of the bend in which they proffer an explanation that the increase in the liquid film thickness in the inside of the bend is as a result of the effect of gravity and secondary flow existing in the gas phase.

Sakamoto et al. [34] performed experimental work in a horizontal 180° bend using air–water as the working fluids. The diameter and radius of curvature of the bend are 24 mm and 135 mm, respectively. They employed the conductance type probe to measure the liquid film thickness and an L-shaped stainless steel sampling tube to measure the local droplet flow rate. They reported the distribution of annular liquid film thickness and the local drop flow rate in the gas core in a straight pipe and at the end of the U-bends at horizontal to horizontal (upward), vertical upward, 45° upward to the horizontal.

Chong et al. [12] also calculated the liquid film thickness in a 150 mm internal diameter U-bend and inverted U-bend which was used to join vertical straight pipes to form a serpentine pipeline. Their aim basically was to calculate the conditions at which dry-out occurs in the serpentine channels of fired reboilers.

Tkaczyk and Morvan [39] used finite volume-based CFD model to predict liquid film thickness in an annular two-phase flow around a C-bend. The liquid film thickness was explicitly solved using a modified Volume of Fluid (VOF) method while the droplets were traced using a Lagrangian technique. They explained that the entrained droplets interact with the liquid film whenever they contact the film surface and they used the Weber number to characterise the regime of impingement (stick, rebound, spread and splash). They concluded that the deposition of entrained droplets and secondary flow which occurs in the gas phase has a strong influence on the liquid film thickness distribution in annular flow.

Almabrok et al. [5] studied experimentally gas–liquid two-phase flow behaviours in upward and downward vertical pipes connected to a 180° bend with serpentine configurations using wire mesh sensor (WMS) and liquid film thickness probes. They used the WMS to obtain void fraction distribution while the circumferential profile of the liquid

film thickness at different axial positions along both sections were obtained using the liquid film thickness probes. In their study, they concluded that in the downward flow, the liquid film thickness is thicker at 90° of the top position than other locations for the whole range of the superficial velocities tested which is as a result of the centrifugal force that tends to push the liquid into the outer curvature of the bend. Also, for the upward position, the liquid film thickness distribution at the top, middle and bottom positions is symmetrically circumferentially uniform. However, the liquid film thickness at the bottom position was notably thicker than those at the top and middle positions. Abdulkadir et al. [4] carried out experimental measurement of liquid film distribution of an air–water mixture flowing through a vertical 180° return bend using flush mounted pin probes and parallel wire probes. In their experiment, a bend of internal diameter of 127 mm and a curvature ratio (R/D) of 3 were used. The range of superficial velocities for both the gas and liquid phases are 3.5–16.1 m/s and 0.02–0.2 m/s, respectively, and from their experimental results, they concluded that the average liquid film thickness peaked at 90° corresponding to liquid and gas superficial velocities of 0.02 m/s and 6.2 m/s, respectively. Also, from the result of their polar plots of the averaged liquid film thickness in the bend, they observed that the distribution of the liquid film thickness is not symmetrical with thicker films on the inside of the bend due to the action of gravity.

Liu and Liu [26] estimated sand erosions in elbows for annular–mist flow based on liquid film thickness and droplet diameter using a numerical method. In their work, they used two liquid film thickness correlations and three droplets mean diameter prediction models to compare calculated results with experimental data available in the literature. They were also able to develop numerical prediction procedure based on the information of the liquid film thickness and droplet diameter verification. From the results obtained, they concluded that Henstock and Hanratty [22]’s liquid film thickness correlation is more efficient and that the droplet diameter model of Kocamustafaogullari et al. [24] is the most accurate.

2.5. Liquid film thickness prediction model for gas–liquid flow in a 90° elbow

The presence of elbows, especially the 90° type, plays a very important role in changing the fluid flow direction in pipelines which finds applications in process industries especially in the oil and gas sector. Over the years, a number of research works have been carried out to study the behaviour of fluid across the 90° bend and how the hydrodynamic parameters are affected as a result of the bend. In the literature, a bulk of the research effort is concentrated mainly on the study of the pressure drop and erosion-corrosion effect as a result of the 90° elbow, but work on the study of the liquid film thickness across the 90° are quite scarce.

For example, Barton [10] gave an overview of the erosion mechanisms in elbows in hydrocarbon production systems, Ansari et al. [8] studied the two-phase gas–liquid/solid flow modelling in 90° bends and its effect on corrosion. Droubi et al. [17] used CFD to analyse sand erosion in a 90° sharp bend geometry. For the study on pressure drop, Spedding and Benard [38] studied the gas–liquid two phase flow through a vertical 90° elbow bend where they reported pressure drop data for the two-phase air–water flow. Sanchez-Silva et al. [35] performed an evaluation of the pressure drop models for two-phase flow in a 90° bend. Mazumder [28] used CFD to analyse the effect of the elbow radius on pressure drop in a multiphase flow.

For the liquid film thickness across the 90° elbow, very limited information exists in the literature. Abdulkadir et al. [4] carried out experimental investigation on liquid film thickness behaviour within a large diameter vertical 180° return bend. They were able to establish a relationship between the liquid film thickness and the 45°, 90° and 135° bends locations. They discovered that at liquid and gas superficial velocities of 0.02 m/s and 6.2 m/s, respectively, the average liquid film

thickness can be observed to peak at 90° bend location due to the fact that at this location, the effect of gravity is more pronounced and as such drains the liquid to the bottom of the pipe. In order to use such important observation reported by Abdulkadir et al. [4] and other researchers on the relationship between the liquid film thickness and the angle of the elbow for design purposes, it is important to develop a correlation that gives a true representation of what goes on within such flow systems. In the literature and to the best of our knowledge, the only model correlation that captures the relationship between the liquid film thickness and other hydrodynamic flow parameters across a 90° elbow is the one developed by Zahedi et al. [46]. They used a pipe with an internal diameter of 76.2 mm and a length of 0.762 m which was connected to a 114.3 mm radius of curvature and another straight section of pipe of 152.4 mm in length. Experimental data at 45° elbow were used to develop a new correlation to predict the liquid film thickness along the outer walls of the elbow. The new correlation is given as:

$$\delta^+ = 3 \times 10^{-9} Re_{lf}^{2.71} Re_{if} > 1000 \quad (12)$$

The correlation is actually based on the work of Kosky [25], Asali et al. [9], and Ambrosini et al. [6]. It is worth mentioning that the work of Kosky was concerned with the determination of the liquid film thickness for vertical upward flows in straight sections of pipes and not across a 90° bend. Also, MacGillivray [27] stated that the correlations of Kosky, Asali and Ambrosini are not very practical for design purposes since they require either the knowledge or calculation of liquid entrainment (to calculate the liquid film mass flow rate) or the shear stress (to calculate the friction velocity). These two quantities are not readily available from experimental work and must be calculated using further empirical or semi-empirical correlations. Also, the correlation developed by Zahedi et al. [46] did not capture the relationship between the centrifugal force and gravitation force which majorly determines the distribution of the phases in the 90° bend. Therefore, there is a need to develop a correlation that can reasonably predict the liquid film thickness from gas and liquid superficial velocities and their physical properties. This work therefore is targeted to develop a new correlation which overcomes the deficiency existing in Zahedi et al. [46] to predict the liquid film thickness at a 90° measuring location in a vertical 180° return bend. The generalization property of the developed correlation will be tested by extending the liquid film thickness prediction to the 45° and 135° bend positions. Finally, the performance of the correlation is evaluated by the data in vertical annular upflow system of MacGillivray [27].

3. Experimental methodology

The experimental investigations were carried out on a large close loop facility available within the Chemical Engineering Laboratories of the University of Nottingham. The facility shown schematically in Fig. 1 has been reported previously by Abdulkadir et al. [3,4]. Details of the experimental set-up can thus be found in Abdulkadir [1] and Abdulkadir et al. [3,4]. However, a brief description of the rig is presented here for sake of completeness.

The stored water in the bottom of the separator was pumped to an air–water mixer before it entered the riser, flowed into the bend, went down the downcomer and finally returned to the separator. The separator is a cylindrical stainless steel vessel of 1 m in diameter and 4 m high filled with 1600 L of water. Air used as the gas phase was driven to the air–water mixer by two liquid-ring-pump compressors powered by two 55 kW motors. The gas flow rates were regulated by varying the speed of the compressor motors (up to 1500 rpm) together with the valves just below the gas flow meters Abdulkadir et al. [4]. The liquid and gas superficial velocities employed were in the ranges from 0.02 to 0.2 m/s and 3.5 to 16.1 m/s, respectively.

Before the commencement of the experiments, the flow loop was

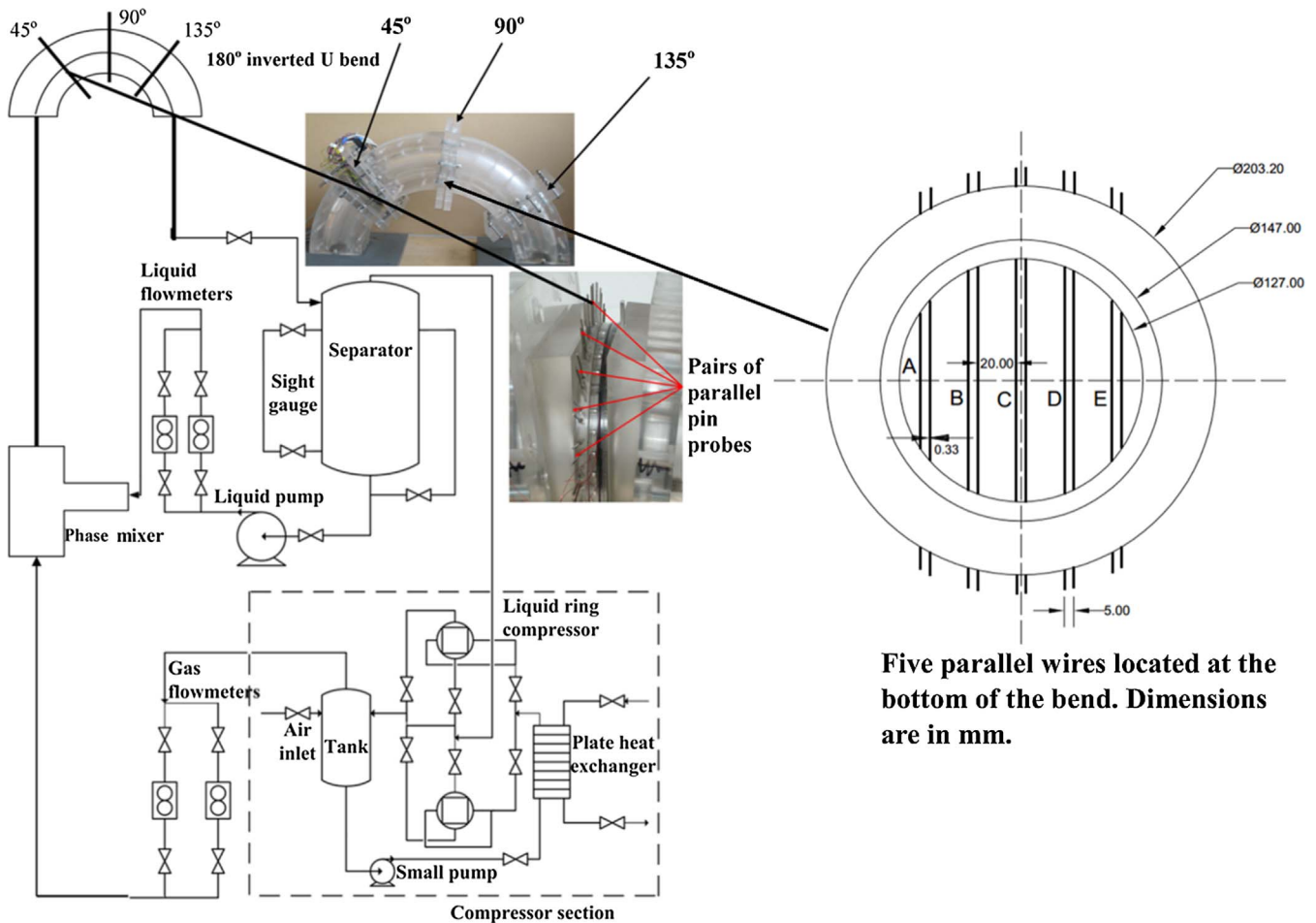


Fig. 1. Schematic diagram of the experimental facility. Adapted from Abdulkadir et al. [4]. The spacing between the two parallel wires of each pair is 5 mm and the distance between pair is 20 mm, with the central pair placed symmetrically about a vertical diameter. The electrodes of the pairs of parallel pin probes were spaced by every 10° from each other and 11.84° from the closest wire probe assembly. The probes were made from 1.5 mm diameter welding rods, made of stainless steel to avoid problems of corrosion.

pressurised to 3 bar (a) using compressed main air.

The two-phase mixture travels for 11 m along a 127 mm internal diameter vertical riser downstream of the mixer in which annular or churn flow is formed. The test bend with the same internal diameter was mounted on top of the riser. The 180° return bend has a radius of curvature of 381 mm ($R/D = 3$) and consist of four modular blocks and one instrumentation section containing all the measuring sensors (parallel-ring probes, parallel-wire probes and flush-mounted pin probes). This modular construction enables the measuring section to be inserted every 45° along the bend as shown in Fig. 1 [4]. After the bend, the air–water flow mixture travels a further 9.6 m vertically downwards in a downcomer and 1.5 m horizontally to the separator where the gas and the liquid are separated and directed back to the compressors and the pump respectively, to create a double closed loop.

Liquid film thickness measurements were carried out using a conductance technique, which employed either flush mounted or parallel wire probes. The first type was used for the almost entire section of the pipe while the second type, suitable for higher liquid film thickness, was used only for the bottom section of the bend. The parallel-wire probes used to measure liquid film thickness at the bottom of the bend are the same type employed by Conte [14], Conte and Azzopardi [15], Geraci et al. [21] and Abdulkadir et al. [4]. In this methodology, five pairs of stainless steel wires are stretched along chords of the pipe cross-section and the resistance between pairs measured. On the other hand, the flush mounted pin probes was used for very thin liquid films, typically up to 2.5 mm. Details can be found in Abdulkadir [1] and Abdulkadir et al. [4].

4. Correlation development

The liquid film thickness correlation was based on the present experimental data in an inverted 180° degree return bend.

According to Ju [23], liquid film thickness is a function of gas and liquid superficial velocities, gas and liquid fluid properties and pipe diameter. Contrary to the assumption of many researchers such as Berna et al. [11], Asali et al. [9], Sawant [36] and Fukano and Furukawa [18] that the effect of liquid velocity on the liquid film thickness is directly reflected in a function of the liquid Reynolds number, Ju [23] reported that the liquid velocity effect is more appropriately described by the liquid Weber number (We). He concluded that the surface tension force is more important than the viscosity force during the interaction of the two phases. This claim is supported by the fact that the liquid Reynolds number failed to converge data taken from different pipe diameters whereas the Weber number did without introducing new parameters on the diameter as can be seen in Fig. 2.

Another reason that Weber number is better suited for the prediction of the liquid film thickness than the Reynolds number can be understood from the underlined physics in gas-liquid annular flow. The mechanism governing the liquid film thickness in annular flow is the liquid and gas inertia forces over the surface tension. The inertia forces tend to change the shape of the interface while the surface tension tends to keep the shape of the interface. These two mechanisms often compete with each other on the interface shape. The parameter that can represent the inertia force over the surface tension force is the Weber Number.

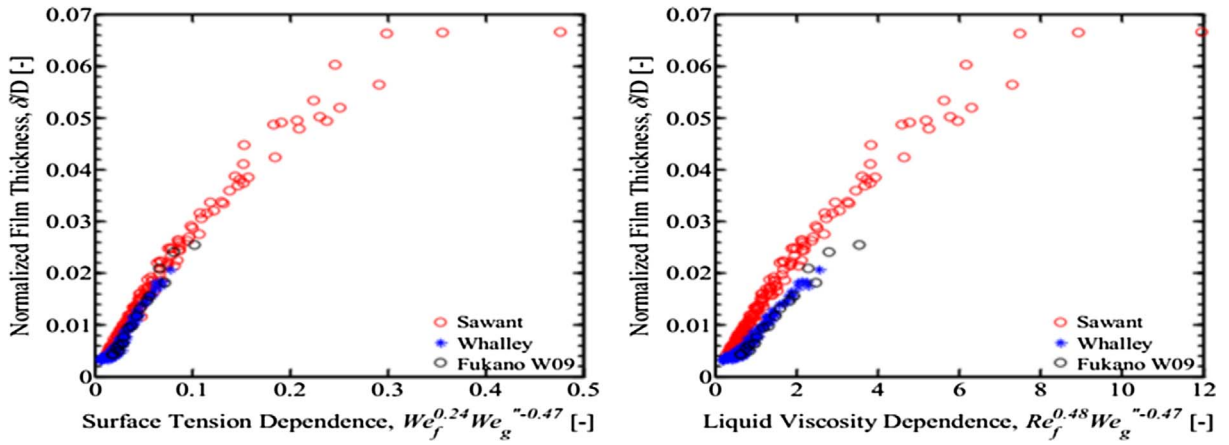


Fig. 2. Liquid velocity effect on film thickness with dependence on surface tension and liquid viscosity [23].

Thus, this work uses Weber number rather than Reynolds number adopted in Zahedi et al. [46] to quantify the liquid film thickness. The Weber numbers for the liquid and gas phases were defined by Eqs. (13) and (14), respectively:

$$We_L = \frac{\rho_L u_{SL}^2 D}{\sigma} \quad (13)$$

The Sawant [36]’s modified Weber Number that accounts for pressure effect is given as:

$$We_G = \frac{\rho_G u_{SG}^2 D}{\sigma} \left(\frac{\Delta\rho}{\rho_G} \right)^{1/4} \quad (14)$$

where

ρ_G is the gas density, D is the pipe diameter and σ is the surface tension, $\Delta\rho$ is the density difference.

Because the flow considered in this work is a vertical churn–annular flow at a 90° elbow measurement location, there was a need to thoroughly understand the forces at play in determining the distribution of the phases within the bend. Abdulkadir et al. [2] as depicted in Fig. 3 had earlier observed that the centrifugal and gravity forces play a significant role in determining the relative positions of the liquid and gas

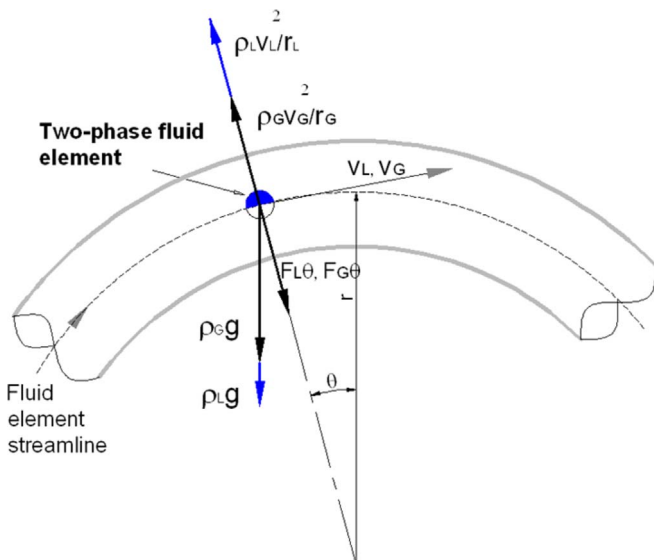


Fig. 3. A schematic diagram showing the interplay between the forces acting on the flow in a 180° return bend.

phases across the radial direction of the bend. Oshinowo and Charles [30] and Usui et al. [41,42] gave a qualitative discussion on the interaction between centrifugal force and gravity for a flow along a bend axis. They explained this interaction by proposing a modified form of Froude’s number expressed in terms of the actual velocities for both the liquid and gas. They achieved this by assuming that the interfacial and frictional forces are negligible when compared with pressure, centrifugal and gravitational forces. They carried out a material balance on the fluid elements in the direction normal to that of the flow at a point in the bend to yield:

$$F_\theta = \text{Pressure force} + \text{kinetic energy force} + \text{gravity force} \quad (15)$$

For liquid phase,

$$F_{L\theta} = \text{Pressure force} + \frac{\rho_L v_L^2}{r} - \rho_L g \sin\theta \quad (16)$$

For gas phase,

$$F_{G\theta} = \text{Pressure force} + \frac{\rho_G v_G^2}{r} - \rho_G g \sin\theta \quad (17)$$

where $F_{L\theta}$ and $F_{G\theta}$ are the net forces of the liquid and gas phases, respectively.

At equilibrium, $F_{L\theta} = F_{G\theta}$, \Rightarrow Eq. (16) = (17)

$$\frac{\rho_L v_L^2}{r} - \rho_L g \sin\theta = \frac{\rho_G v_G^2}{r} - \rho_G g \sin\theta \quad (18)$$

In order to simplify Eq. (18), two cases will need to be considered:

Case 1: Horizontal flow; $\theta = 0^\circ$ or 180° $\sin\theta = 0$, gravity forces becomes zero.

Thus, Eq. (18) reduces to

$$\frac{\rho_L v_L^2}{r} = \frac{\rho_G v_G^2}{r} \Rightarrow \frac{\rho_G v_G^2}{\rho_L v_L^2} = 1 \quad (19)$$

Thus,

$$\frac{\rho_G v_G^2}{\rho_L v_L^2} = Fr_\theta \quad (20)$$

Case 2: Elevated flow; $\theta \neq 0^\circ$ or $\theta \neq 180^\circ \Rightarrow \sin\theta \neq 0$

Eq. (18) can be rearranged as

$$\frac{\rho_L v_L^2}{r} - \frac{\rho_G v_G^2}{r} = \rho_L g \sin\theta - \rho_G g \sin\theta \quad (21)$$

Dividing through Eq. (21) by $\rho_L g \sin\theta$, we have

$$\frac{v_L^2}{rg \sin\theta} - \frac{\rho_G v_G^2}{rg \rho_L \sin\theta} = 1 - \frac{\rho_G}{\rho_L} \quad (22)$$

Eq. (22) can be rearranged as

$$\frac{v_L^2}{rg\sin\theta} \left[1 - \frac{\rho_G v_G^2}{\rho_L v_L^2} \right] = \frac{\rho_L - \rho_G}{\rho_L} \quad (23)$$

Dividing both sides of Eq. (23) by $\frac{\rho_L - \rho_G}{\rho_L}$

$$\frac{v_L^2}{\left(\frac{\rho_L - \rho_G}{\rho_L}\right)rg\sin\theta} \left[1 - \frac{\rho_G v_G^2}{\rho_L v_L^2} \right] = 1 \quad (24)$$

Recall that at radial equilibrium, $F_{L\theta} = F_{G\theta}$ and $Fr_\theta = 1$

The modified form of Froude number becomes Eq. (25) for all cases, that is, $F_{L\theta} > F_{G\theta}$, $F_{L\theta} = F_{G\theta}$, $F_{L\theta} < F_{G\theta}$.

$$\frac{v_L^2}{\left(\frac{\rho_L - \rho_G}{\rho_L}\right)rg\sin\theta} \left[1 - \frac{\rho_G v_G^2}{\rho_L v_L^2} \right] = Fr_\theta \quad (25)$$

In agreement with the explanation put forward by Gardner and Neller [20], Oshinowo and Charles [30] and Usui et al. [41,42] that if the left-hand side of Eq. (25) is greater than 1, then the liquid will move to the outside of the bend and that if less than 1, the liquid will move to inside the bend.

However, Eq. (25) is not very practical for design purposes since it requires either the knowledge or calculation of liquid holdup or void fraction to calculate the liquid velocity. In order to circumvent this challenge, Eq. (26) which is similar to Eq. (25) originally proposed by Gardner and Neller [20] and applied by Abdulkadir et al. [2] and Saidj et al. [33] will be used in this work.

$$Fr_\theta = Fr_G = \frac{u_{SG}}{\sqrt{rg\sin\theta}} = \frac{u_{SG}^2}{rg\sin\theta} \quad (26)$$

Since the modified Weber and Froude numbers can adequately capture the underlined physics of the flow in a bend, the model for the prediction of the liquid film thickness across a 90° elbow location can be proposed as:

$$\delta = C (We_L)^a (We_G)^b (Fr_G)^d \quad (27)$$

where δ is the liquid film thickness, We_L , and We_G are the modified Weber Number for the liquid and gas, respectively, Fr_G is the gas Froude Number, C is an empirical constant, a , b and d are numbers that describe the nature of the relationship between the liquid film thickness and the dimensionless numbers.

One of the attractive features in the proposed model is the fact that most of the important variables that affect the liquid film thickness such as the velocities of the liquid and gas phases, the diameter of the pipe, the physical properties of the phases, and the bend angle are all considered within the model and all these parameters are easily accessed.

In order to determine the values of the empirical constants C , a , b and d , the method of Ju [23] was adapted. The method of Ju [23] involves making a graphical plot of left hand side with each of the dimensionless groups on the right-hand side using a power law relationship in order to obtain the associated empirical constants (different exponents). But in this work, we did not just stop at obtaining the empirical constants, C , a , b and d obtained from the plots. But rather used the empirical constants as initial values in a curve fitting program in Excel called Solver to determine the actual values of these constants. The mathematical basis of the Solver is the minimization of the sum of chi square.

Once the empirical constants are obtained, the model will be tested using experimental data for the 90° bend position.

In order to check the robustness of the newly developed correlation, it was extended to the prediction of the liquid film thickness at bend positions 45° and 135°. It was also evaluated by the published data in MacGillivray [27] for vertical annular upflow to determine its level of accuracy in predicting liquid film thickness.

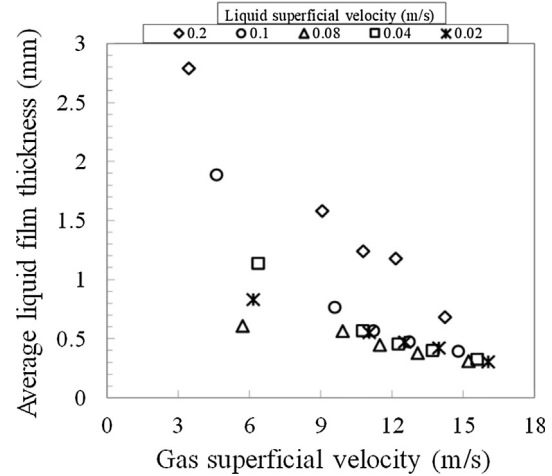


Fig. 4. A plot of the effect of gas superficial velocity on averaged liquid film thickness at constant superficial liquid velocity.

5. Results and discussion

A new proposed liquid film thickness correlation for annular flow in a 180° return bend based on experimental data obtained from a wide range of operating conditions will be presented, analysed and discussed. The liquid superficial velocities ranges from 0.02 to 0.2 m/s and gas superficial velocities from 3.5 to 16 m/s at different measurement locations of 45°, 90° and 135° of the bend with a diameter of 127 mm.

5.1. Dependence of average liquid film thickness on the gas superficial velocity

Fig. 4 shows the relationship between the experimental average liquid film thickness and the gas superficial velocity at constant liquid superficial velocity.

From Fig. 4, the general trend is that the average liquid film thickness decreases as the gas superficial velocity increases at constant liquid superficial velocity as observed by researchers such as Fukano and Furukawa [18], Sawant [36] and Abdulkadir et al. [4]. The explanation for this phenomenon is the formation of the liquid droplets known as droplet entrainment within the gas core as the gas superficial velocity increases.

5.2. Dependence of the average liquid film thickness on the modified liquid Weber number

From Fig. 5, it can be observed that as the modified liquid Weber Number increases, the inertia for the liquid phase increases which

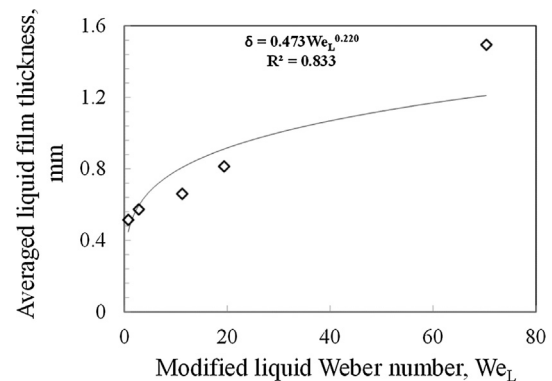


Fig. 5. The relationship between the average liquid film thickness and modified liquid Weber Number.

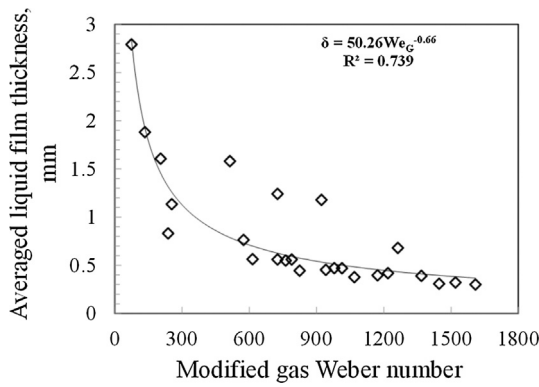


Fig. 6. The relationship between the average liquid film thickness and modified gas Weber Number.

moves more of the liquid into the test region resulting to the increase in the liquid film thickness. This is in agreement with the observation reported by Ju [23].

5.3. Dependence of the average liquid film thickness on the modified gas Weber number

Fig. 6 reveals explicitly the relationship between the average liquid film thickness and the modified gas Weber Number.

It can be deduced from the figure that the liquid film thickness decreases asymptotically as the modified Weber Number increases, meaning that the inertial force which is as a result of an increase in the modified Weber Number due to an increase in the gas superficial velocity, tends to decrease the liquid film thickness.

5.4. Dependency of the average liquid film thickness on the modified Froude number

Fig. 7 shows the relationship between the average liquid film thickness and the modified Froude Number. This dimensionless number is so important in describing the phase distribution of the flow across the bend.

Also from the plot, it can be seen that the average liquid film thickness decreases as the modified Froude Number increases. In summary, the relationship between the averaged liquid film thickness and the various dimensionless numbers can be seen below:

For the liquid phase Weber Number:

$$\delta = 0.473(We_L)^{0.22} \tag{28}$$

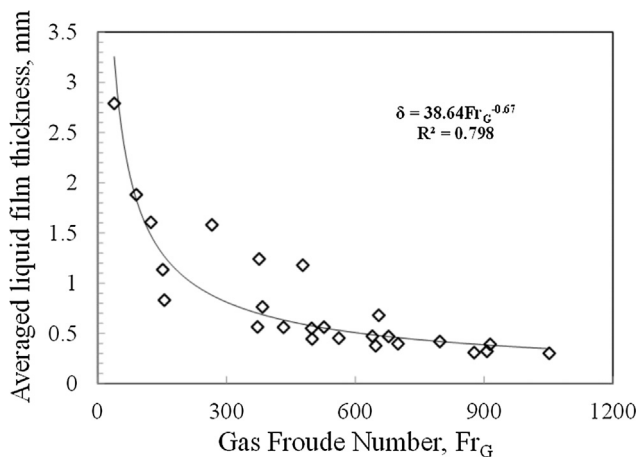


Fig. 7. The relationship between the average liquid film thickness and modified Froude Number.

For the gaseous phase Weber Number:

$$\delta = 50.26(We_G)^{-0.66} \tag{29}$$

For the Froude Number of the gas flow:

$$\delta = 38.64(Fr_G)^{-0.67} \tag{30}$$

Combining all the dimensionless numbers, the new correlation will be:

$$\delta = 918.5879(We_L)^{0.22}(We_G)^{-0.66}(Fr_G)^{-0.67} \tag{31}$$

Comparing Eq. (31) with the functional form of Eq. (27), we have C, a, b and d equals 918.5879, 0.22, -0.66 and -0.67, respectively. These values are used as the initial values in an EXCEL program called the SOLVER to determine the actual values which minimizes the error between the actual and predicted values of the liquid film thickness. After several iterations, the converged results that minimizes the value of the error occur when C, a, b, and d are 28.4061, 0.10318, -0.30954 and -0.31423 respectively. The final correlation for the liquid film model can be represented as:

$$\delta = 28.4061(We_L)^{0.10318}(We_G)^{-0.30954}(Fr_G)^{-0.31423} \tag{32}$$

5.5. Comparison of the predicted liquid film thickness with the measured values outside and inside the bend

In this work, the experimental (measured) liquid film thickness inside and outside of the 180° return bend for an air–water churn–annular system at the measurement location of 90° of the bend are compared with those predicted by the correlation in Fig. 8. In general, they have excellent agreement except at low gas superficial velocities for outside and inside the bend and at low and high liquid superficial velocities for inside bend (Fig. 8a and i). At low gas superficial velocities the flow patterns in the bend are believed in the transition of churn to annular flow. It is not surprising that the correlation gives higher deviations. The correlation considerably underestimated the liquid film thickness inside the bend at $u_{SL} = 0.02$ m/s (Fig. 8a) and 0.2 m/s (Fig. 8i). This can be explained because with the increase of u_{SL} more droplets were deposited at inside the bend and the flow patterns deviated from typical annular flow. Overall the correlation gives better prediction to the liquid film thickness outside the bend than the inside one. The correlation is also better suited for predicting annular gas–liquid flow.

5.6. Comparison of the predicted averaged liquid film thickness across the bend with the experimental data

This section shows a comparison between the experimental average liquid film thickness across the bend with the data predicted by the correlation at three measurement locations of 45°, 90° and 135° of the bend.

In Fig. 9, the values of predicted average liquid film thickness at 90° bend measurement location are plotted against the experimental data. Excellent agreement is shown over the entire range of the observations with a Pearson Product-moment correlation coefficient of 88.27%. The Pearson Product-moment correlation coefficient is a measure of the strength of a linear association between two variables. It attempts to draw a line of best fit through the data of two variables [1]. When the correlation was extended to predict the average liquid film thickness at the locations of 40° and 135° of the bend, very good agreements are also found, Figs. 10 and 11. Pearson Product-moment correlation coefficients for the two figures are 93.69% and 82.57%.

5.7. Correlation evaluation by the data available in the literature

The robustness of the correlation developed in this work was evaluated by the liquid film thickness data reported in MacGillivray [27]. Good agreement can be seen from Fig. 12 and that most data points

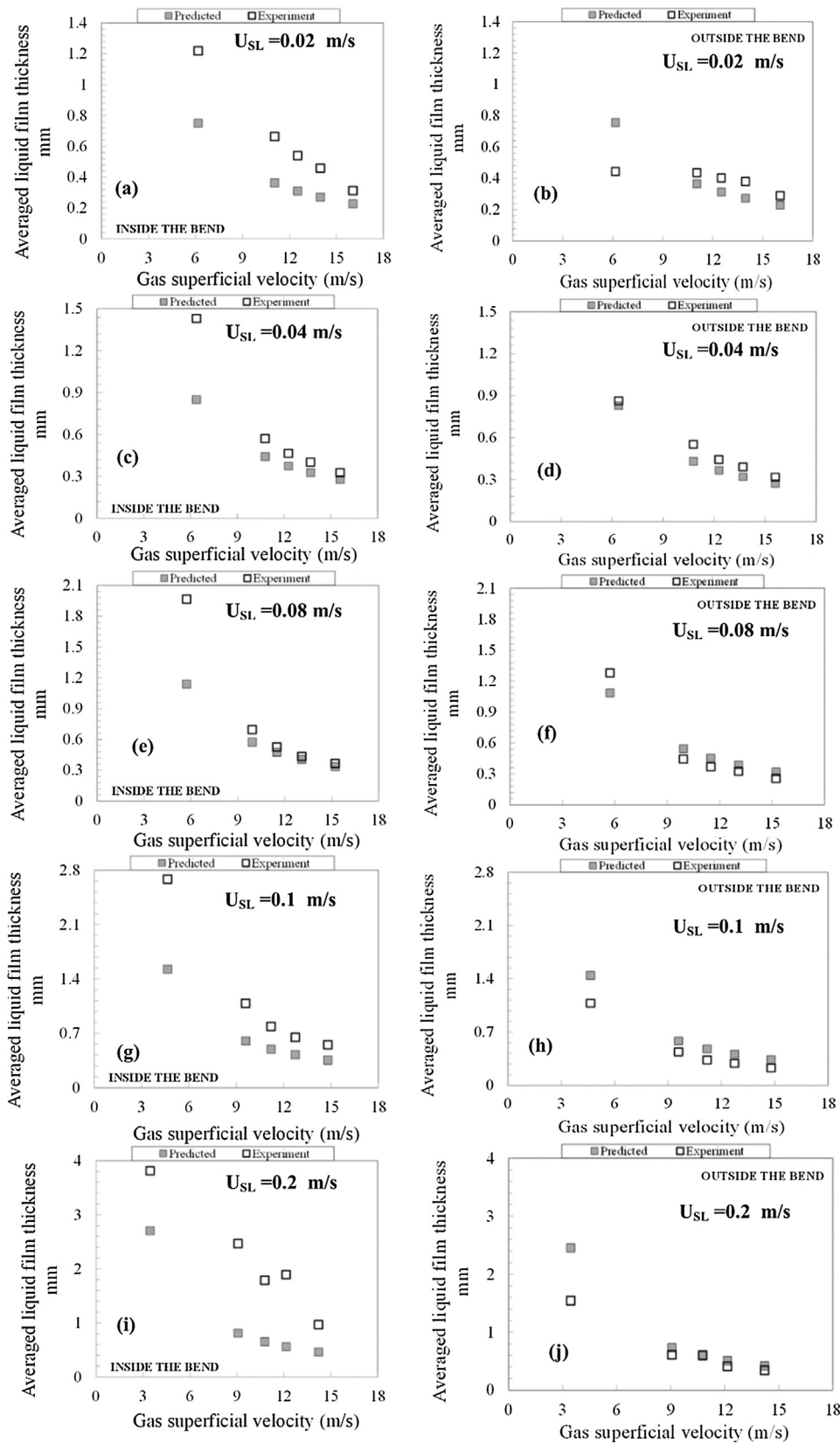


Fig. 8. A plot of the averaged liquid film thickness along the outer and inner bend versus the gas superficial velocity for each of the liquid superficial velocities. 90° bend position.

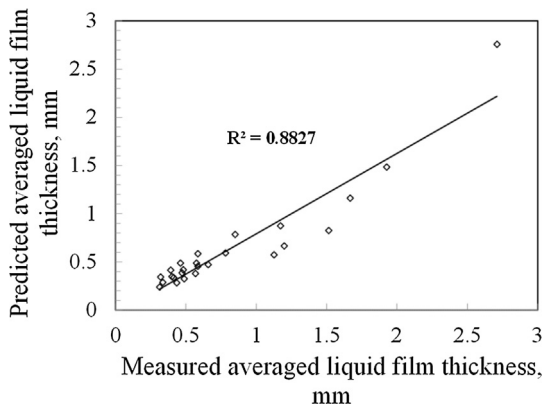


Fig. 9. a plot of comparison between experimental liquid film thickness against predicted liquid film thickness obtained from new developed correlation. 90° bend position (present study).

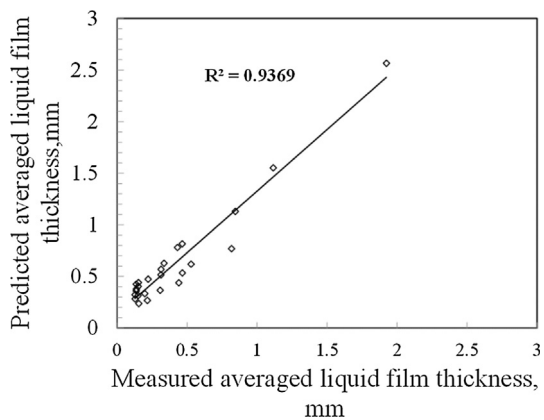


Fig. 10. a plot of comparison between experimental liquid film thickness against predicted liquid film thickness obtained from new developed correlation. 45° bend position.

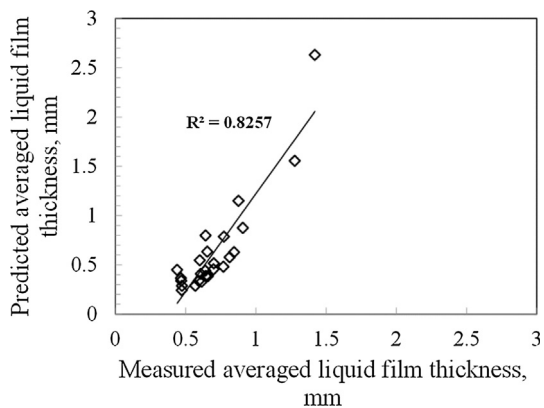


Fig. 11. A plot of comparison between experimental liquid film thickness against predicted liquid film thickness obtained from new developed correlation. 135° bend position.

clustered along the correlation line with a Pearson Product-moment correlation coefficient of 92.01%. We have confidence to believe that the liquid film thickness correlation developed in this work can be successfully applied to air–water and helium–water annular systems with a wide range of pipe diameters.

6. Conclusion

In this work, the prediction of liquid film thickness in a 180° bend under gas–liquid annular conditions was carried out and discussed using experimental data. A liquid film thickness correlation based on

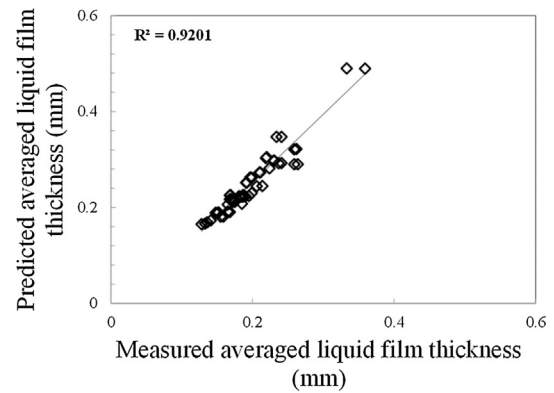


Fig. 12. A plot of the predicted averaged liquid film thickness against the data of MacGillivray [27] for vertical annular pipe flow.

dimensionless numbers which reflect the underlined physics governing gas–liquid interaction in the bend was successfully proposed. Modified liquid and gas Weber Numbers (We_L and We_G) were chosen to be used in the model as the Weber Numbers capture the two important forces (inertial and surface tension forces) which govern the formation of the liquid film thickness within the system. Gas Froude Number was also chosen because it captures the two important forces (Centrifugal and gravitational forces) which determine the distribution of the phases across a bend. It was observed that the relationship between the averaged liquid film thickness and the modified liquid Weber Number is such that as the modified liquid Weber Number increases, the average liquid film thickness also increases. For the modified gas Weber Number, it was observed that as the modified gas Weber Number increases, the average liquid film thickness decreases asymptotically to a minimum value and the same trend was observed for the modified Froude Number.

A new correlation that can predict the liquid film thickness in gas–liquid annular flow was developed ($\delta = 28.4061 (We_L)^{0.10318} (We_G)^{-0.30954} (Fr_G)^{-0.31423}$). Good agreement was found between the predicted values of liquid film thickness with the experimental data at different measuring locations of the bend. Pearson product-moment correlation coefficients for the 45°, 90° and 135° bend locations were 93.69%, 88.27% and 82.57%, respectively. The validation of the proposed correlation used to predict liquid film thickness in gas–liquid annular systems with different pipe diameters were examined against the available data in the literature. Good agreement is found.

Acknowledgment

Abdulkadir, M., would like to express his sincere appreciation to the Nigerian government through the Petroleum Technology Development Fund (PTDF) for providing the funding for his doctoral studies.

This work has been undertaken within the Joint Project on Transient Multiphase Flows and Flow Assurance. The Author(s) wish to acknowledge the contributions made to this project by the UK Engineering and Physical Sciences Research Council (EPSRC) and the following: GL Industrial Services; BP Exploration; CD-adapco; Chevron; ConocoPhillips; ENI; ExxonMobil; FEESA; IFP; Institut for Energiteknikk; PDVSA (INTEVEP); Petrobras; PETRONAS; SPT; Shell; SINTEF; Statoil and TOTAL. The Author(s) wish to express their sincere gratitude for this support.

References

- [1] Abdulkadir, M., 2011. Experimental and Computational Fluid Dynamics (CFD) of Gas–liquid Flow in Bends. PhD thesis, University of Nottingham, United Kingdom.
- [2] M. Abdulkadir, D. Zhao, S. Sharaf, L.A. Abdulkareem, I.S. Lowndes, B.J. Azzopardi, Interrogating the effect of 90° bends on air–silicone oil flows using advanced

- instrumentation, *Chem. Eng. Sci.* 66 (2011) 2453–2467.
- [3] M. Abdulkadir, D. Zhao, A. Azzi, I.S. Lowndes, B.J. Azzopardi, Two-phase air–water flow through a large diameter vertical 180° return bend, *Chem. Eng. Sci.* 79 (2012) 138–152.
- [4] M. Abdulkadir, A. Azzi, D. Zhao, B.J. Azzopardi, Liquid film thickness behaviour within a large diameter vertical 180° return bend, *Chem. Eng. Sci.* 107 (2014) 137–148.
- [5] Almabrok, A.A., Lao, L., Yeung, H., 2013. Effect of 180° bends on gas/liquid flows in vertical upward and downward pipes. *J. Comput. Methods Multiphase Flow* 79, ISSN 1743-3533 (on-line).
- [6] W. Ambrosini, P. Andreussi, B.J. Azzopardi, A physically based correlation for drop size in annular flow, *Int. J. Multiph. Flow* 17 (1991) 497–507.
- [7] Anderson, G.H., Hills, P.D., 1974. Two-phase annular flow in tube bends. Symposium on Multiphase Flow Systems, University of Strathclyde, Glasgow, Paper J1. Published as Institution of Chemical Engineers Symposium, Series No. 38.
- [8] Ansari, M.R., Mohammadi, S., Oskouei, M.K., 2012. Two phase gas/liquid–solid flow modelling in 90° bends and its effect on erosion. *Glob. J. Res. Eng. Mech. Mech. Eng.* 12.
- [9] J.C. Asali, T.J. Hanratty, P. Andreussi, Interfacial drag and film height for vertical annular flow, *AIChE J.* 31 (1985) 895–902.
- [10] Barton, N.A., 2003. Erosion in elbows in hydrocarbon production systems: review document. Health and Safety Executive.
- [11] C. Berna, A. Escriva, J.L. Munoz-Cobo, L.E. Herranz, Review of droplet entrainment in annular flow: interfacial waves and onset of entrainment, *Prog. Nucl. Energy* 74 (2014) 14–43.
- [12] L.Y. Chong, B.J. Azzopardi, D.J. Bate, Calculation of conditions at which dryout occurs in the serpentine channels of fired reboilers, *Chem. Eng. Res. Des.* 83 (2005) 412–422.
- [13] C. Chung, D. Choi, J.M. Kim, K.H. Ahn, S.J. Lee, Numerical and experimental studies on the viscous folding in diverging microchannels, *Microfluid. Nanofluid.* 8 (2010) 767–776.
- [14] G. Conte, An experimental study for the characterisation of gas/liquid flow splitting at T-junctions, PhD thesis University of Nottingham, 2000.
- [15] G. Conte, B.J. Azzopardi, Film thickness variation about a T-junction, *Int. J. Multiph. Flow* 29 (2003) 305–325.
- [16] de Jong, P.A., 1999. An investigation of film structure and pressure drop in microgravity annular flow, MSc. Thesis, University of Saskatchewan, Saskatoon.
- [17] Droubi, M.G., Tebowei, R., Islam, S.Z., Hossain, M., Mitchell, E., 2016. CFD analysis of sand erosion in 90° sharp bend geometry. In: Proceedings of the 9th International Conference on Computational Fluid Dynamics (ICCFD 9) Istanbul, Turkey.
- [18] T. Furukawa, T. Furukawa, Prediction of the effects of liquid viscosity on interfacial shear stress and frictional pressure drop in vertical upward gas-liquid annular flow, *Int. J. Multiph. Flow* 24 (1998) 587–603.
- [19] T. Furukawa, T. Furukawa, Effect of liquid viscosity of flow patterns in vertical upward gas–liquid two phase flow, *Int. J. Multiph. Flow* 27 (2001) 1109–1126.
- [20] G.C. Gardner, P.H. Neller, Phase distribution flow of an air–water mixture round bends and past obstructions, *Proc. Inst. Mech. Engr.* 184 (3C) (1969) 93–101.
- [21] G. Geraci, B.J. Azzopardi, H.R.E. Van Maanen, Inclination effects on circumferential film distribution in annular gas/liquid flows, *AIChE J.* 53 (2007) 1144–1150.
- [22] W.H. Henstock, T.J. Hanratty, The interfacial drag and the height of the wall layer in annular flows, *AIChE J.* 22 (1976) 990–1000.
- [23] Ju, P., 2015. Annular flow liquid films dynamics in pipes and rod bundles. PhD thesis, Purdue University, USA.
- [24] Kocamustafogullari, G., Smits, S., Razi, J., and Huang, W., 1993. Droplet size modelling in annular flow. In: Proceedings of the 6th International Topical Meeting on Nuclear Reactor Thermal Hydraulics.
- [25] P.G. Kosky, Thin liquid films under simultaneous shear and gravity forces, *Int. J. Heat Mass Transf.* 14 (8) (1971) 1220–1224.
- [26] Liu, M., Liu, H., 2015. A Numerical procedure to estimate sand erosion in elbows for annular-mist flow based on film thickness and droplet diameter prediction. In: 25th International Ocean and Polar Engineering Conference, Hawaii, USA, ISOPE-15-299.
- [27] MacGillivray, R.M., 2004. Gravity and Density Effects on Annular Flow Average Film Thickness and Frictional Pressure Drop. Msc Thesis, University of Saskatchewan.
- [28] Mazumder, Q.H., 2012. CFD analysis of the effect of elbow radius on pressure drop in multiphase flow. *J. Model. Simulat. Eng.* Article I.D. 125405.
- [29] P.M. Oliveira, J.R. Barbosa, Developing air–water flow downstream of a vertical 180° return bend, *Int. J. Multiph. Flow* 67 (2014) 32–41.
- [30] T. Oshinowo, M.E. Charles, Vertical two-phase flow-Part 1: Flow pattern correlations, *Can. J. Chem. Eng.* 52 (1974) 25–35.
- [31] M. Parsi, M. Agrawal, V. Srinivasan, R.E. Vieira, C.F. Torres, B.S. McLaury, S.A. Shirazi, CFD Simulation of sand particle erosion in gas-dominant multiphase flow, *J. Nat. Gas Sci. Eng.* 27 (2015) 706–718.
- [32] A.M. Ribeiro, Studies of Gas–liquid Flow in Bends, PhD Thesis University of Birmingham, United Kingdom, 1993.
- [33] Saidj, F., Kibboua, R., Azzi, A., Ababou, N. and Azzopardi, B.J., 2014. Experimental investigation of air–water two-phase flow through vertical 90° bend. *Exp. Therm. Fluid Sci.* 57, 226–234.
- [34] Sakamoto, G., Doi, T., Murakami, Y., and Usui, K., 2004. Profiles of liquid film thickness and droplet flow rate in U-bend annular mist flow. In: 5th International Conference on Multiphase Flow, ICMF 2004, Japan, May 30–June 4.
- [35] S. Sanchez-Silva, J.C. Luna Resendiz, I. Carvajal Mariscal, R. Tolentino Eslava, Pressure drop models evaluation for two-phase flow in 90° horizontal elbows, *Ingenieria Mecanica Tecnologia Y Dessorolo* 3 (4) (2010) 115–122.
- [36] Sawant, P., 2008. Dynamics of Annular Two-phase Flow. Ph.D. thesis. Purdue University, West Lafayette, USA.
- [37] D. Schubring, A. Ashwood, T. Shedd, E. Hurlburt, Planar Laser-induced fluorescence (PLIF) measurements of liquid film thickness in annular flow. Part I: Methods and data, *Int. J. Multiph. Flow* 36 (10) (2010) 815–824.
- [38] P.L. Spedding, E. Benard, Gas–liquid two-phase flow through a vertical 90° elbow bend, *Exp. Therm Fluid Sci.* 31 (2007) 761–769.
- [39] T.M. Tkaczyk, H.P. Morvan, Film thickness prediction in an annular two-phase flow around C-shaped bend, *J. Comput. Multiphase Flows* 3 (2011) 27–39.
- [40] P.M. Tkaczyk, H.P. Morvan, Film thickness prediction in an annular two-phase flow around C-shape bend, *J. Comput. Multiphase Flows* 3 (2010) 27–39.
- [41] K. Usui, S. Aoki, A. Inoue, Flow behaviour and phase distributions in two-phase flow around inverted U-bend, *J. Nucl. Sci. Technol.* 20 (1983) 915–928.
- [42] K. Usui, S. Aoki, A. Inoue, Flow behaviour and pressure drop of two-phase flow through C-shaped bend in a vertical plane-I: Upward flow, *J. Nucl. Sci. Technol.* 17 (1980) 875–887.
- [43] C.C. Wang, I.Y. Chen, Y.W. Yang, Y.J. Chang, Two-phase flow pattern in small diameter tubes with the presence of horizontal return bend, *Int. J. Heat Mass Transf.* 46 (2003) 2976–2981.
- [44] C.C. Wang, I.Y. Chen, Y.W. Yang, R. Hu, Influence of horizontal return bend on the two-phase flow pattern in small diameter tubes, *Exp. Therm Fluid Sci.* 28 (2004) 145–152.
- [45] Wang, C.C., Chen, I.Y., Lin, Y.T., Chang, Y.J., 2008. A visual observation of the air–water two-phase flow in small diameter tubes subject to the influence.
- [46] Zahedi, P., Vieira R.E., Shirazi S.A., McLaury, B.S., 2016. Liquid film thickness and erosion of elbows in gas–liquid annular flow, In: CORROSION 2016, Houston-Texas, 7711.